P3.13 THERMODYNAMIC AND KINEMATIC ANALYSIS NEAR AND WITHIN THE TIPTON, KS TORNADO ON MAY 29 DURING TWISTEX 2008

Bruce D. Lee and Catherine A. Finley

WindLogics, Inc.
Grand Rapids, Minnesota

Tim M. Samaras
Applied Research Associates, Inc.

1. INTRODUCTION

During the Tactical Weather-Instrumented Sampling in/near Tornadoes Experiment (TWISTEX) a mobile mesonet (Straka et al. 1996) and array of in situ probes (Samaras and Lee 2003) collected data both within the near-tornado environment and in the tornado that occurred near Tipton, Kansas on 29 May 2008. The tornado sampled was just one of many tornadoes produced by its parent supercell. The TWISTEX teams on this evening observed a nearly continuous cycle of tornadogenesis and decay up to nightfall. The data collection on May 29 was unique with regard to sampling the near-surface thermodynamic conditions within a tornado while simultaneously sampling the thermodynamic and kinematic conditions just external to a tornado and within the broader supercell rear-flank downdraft (RFD) outflow. With one in situ probe centered along the tornado path, another probe on the edge of the circulation, one mesonet station just 200-300 meters south of the tornado and another mesonet station approximately 1 km south of the tornado, this rare dataset provides an opportunity to determine the thermodynamic character of the flow getting ingested into the tornado from the RFD outflow along the right flank (looking downstream) of the tornado.

One of the primary objectives of the field portion of TWISTEX was to gather thermodynamic and kinematic data with a mobile mesonet in the RFD outflow region near tornadoes and the adjacent RFD gust front region, and with in situ probes in or very near tornadoes. The sampling goal is designed such that a combined thermodynamic and kinematic mapping can be done in the tornadogenesis and tornado maintenance regions while also addressing project objectives involving near-surface tornadic flow field analysis. While a considerable number of mobile mesonet RFD datasets have been analyzed to determine the association between RFD thermodynamic character and the tornadic nature of a supercell (Markowski 2002, Markowski et al. 2002 (hereafter MSR2002), Lee et al. 2004; Finley and Lee 2004, Grzych et al. 2007 (hereafter GLF2007), Hirth et al. 2008) there exists only a few RFD outflow mesonet datasets with good sampling within close range of a tornado, and no viable datasets where both mobile mesonet and in situ tornado data exists. Further, while the number of analyzed RFD events sampled by mobile mesonets for tornadic and non-tornadic supercells (e.g., MSR2002) is significant, it is far from exhaustive given the latitude of the potential scenarios leading to tornadogenesis and tornadogenesis failure, and especially with respect to focused sampling on regions hypothesized to be crucial for understanding tornadogenesis and maintenance.

TWISTEX was carried out from early May through mid-June of 2008 with a domain that included regions from the upper Midwest through the southern Great Plains. The project had a typical compliment of 3 mobile mesonet vehicles and a probe vehicle that transported both thermodynamic probes and a photogrammetric probe (see Karstens et al. 2008 for images of the project's observational platforms). Undergraduate and graduate participants were mainly from the atmospheric and meteorology programs at Iowa State University and Metropolitan State College of Denver.

2. DATA COLLECTION AND METHODOLOGY

TWISTEX teams initially targeted a promising environment for tornadic supercells in southern/central Nebraska on the May 29th. While tornadic supercells were indeed present along and near I-80 with Kearney incurring considerable tornado damage (*National Climatic Data Center*), the convective evolution away from isolated cells

Corresponding author address: Dr. Bruce D. Lee
WindLogics, Inc. – Itasca Technology Center
Grand Rapids, MN 55744
email: blee@windlogics.com

and toward high precipitation supercell structures compromised the deployment opportunities. Upon observing more isolated convective initiation ongoing in western/northwestern Kansas, TWISTEX teams promptly dropped south in anticipation of engaging the storms in northern Kansas.

The TWISTEX sampling array on May 29th consisted of the probe team with a full compliment of thermodynamic and photogrammetric probes and 2 mobile mesonet stations. The third mobile mesonet platform was unable to participate due to damage from a violent rear-flank downdraft outflow north of Quinter, Kansas on May 23rd (see Finley and Lee 2008, Karstens et al. 2008). The instrumentation and data processing and display software were nearly identical on all mesonet vehicles. The type of instrumentation and mobile mesonet station configuration is similar to that presented by Straka et al. (1996). More recent models of the instrumentation have been used when available. Field procedures were developed such that the GPS could be used for vehicle direction at all times eliminating the need for a flux gate compass. Data were recorded from the mesonet stations every 2 s. To date, both 6 s averaged and non-averaged data have been utilized, depending upon the spatial and temporal scale of the feature being analyzed. The mesonet dataset was quality controlled in a manner consistent with MSR2002 and GLF2007.

Two types of in situ instrumentation were deployed which included two Hardened In situ Tornado Pressure Recorder (HITPR) probes and one photogrammetric probe. Both probes are aerodynamically shaped and engineered to withstand the harsh tornadic environment (Samaras 2004).

The HITPR probes were outfitted with sensors that measure temperature, pressure, and relative humidity, which are recorded at 10 samples per second. All data underwent quality control inspection. The HITPR probes essentially become an integral part of the mesonet in coordinated deployment.

Given the lack of nearby ASOS stations and mesoscale nature of the environment the storms were moving into, the mobile mesonet was utilized to determine the base state used to assess perturbation quantities of thermodynamic variables. A period was selected when the mesonet was sampling air with a thermodynamic character deemed to be representative of the pre-storm environment.

Teams deployed ahead of the target supercell thunderstorm along Kansas Highway 181 approximately 8.5 km northwest of Tipton as shown in Fig. 1. At the radar time depicted in Fig. 1, the probe deployment was nearly complete and the mobile mesonet had previously established positions along the highway. With the storm motions on this day and the road network/conditions available, the deployment strategy was to array all project assets in a north-south array along K-181 and let the targeted supercell features pass over the array.

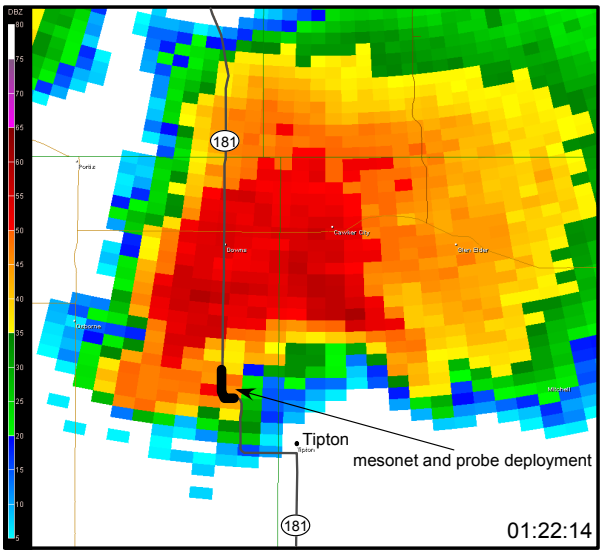

Fig. 1. TWISTEX deployment corridor along K-181 northwest of Tipton. The WSR-88D base reflectivity image at 01:22:14 UTC is from the National Weather Service at Hastings, Nebraska.

3. OBSERVATIONS AND ANALYSIS

Arriving comfortably ahead of the storm's passage over K-181, teams were able to collect inflow observations well ahead the storm's passage over the array. Tornadogenesis was observed at 01:17:40 UTC with a consistent visual condensation cone after 01:18:47 UTC. Figure 2 depicts the tornado's appearance at two key points in the deployment. With the trend in the tornado visual appearance just prior to and following 01:18:53 UTC indicating a non-transient event, and with a reasonably steady track established, both mesonet and probe teams were able to calibrate their positions along K-181 for feature-relative data sampling. Upon arriving at the point along K-181 where the probe director anticipated tornado crossing, the leading edge of the tornado was less than 1 km to the west-southwest with the tornado taking on a considerably wider profile than that observed approximately 3 min earlier (Fig. 2 second panel). The deployment was successful with the tornado passing over the in situ probes

Fig. 2. Visual appearance of the Tipton tornado at 01:18:53 and 01:21:42 UTC. Perspective is looking to the west-southwest in both photographs. (Video capture in bottom panel courtesy of Carl Young).

during the 01:22:45 – 01:23:02 UTC period. The northernmost probe appeared to be in the center of the damage path and measured a 15 mb pressure drop (Karstens et al. 2008) with the southern probe sampling the edge of the tornado.

The leading member of the mobile mesonet, M3, established a position just 200-300 m south of the tornado path and was close enough to be able to sample the inflow into the tornado from the south side. M3 also was close enough to measure a substantial 6-7 mb pressure drop as the circulation passed to the north (see Karstens et al. 2008). M2 sampled positions from 0.5 – 1.0 km south of M3.

Data points were plotted relative to the Hastings, Nebraska National Weather Service WSR-88D radar data using time-to-space conversion as described by MSR2002. This process put the observational mesonet data (mobile mesonet and probe) into the storm's positional frame of reference. The supercell radar echoes were assumed to be in steady state for 5 min periods that approximates the time for a single WSR-88D volume scan. The most important analysis period is shown in Fig. 3, centered on the 01:22:14 UTC base reflectivity scan since the key storm features move over the array within a few minutes either side of this time. As shown in Fig. 3, the mature classic supercell had a fully developed hook. In the prior analysis segment (not shown), the mesonet sampled the RFD gust front passage. Only modest changes in air mass thermodynamics were realized across the initial gust front (detailed later in this section), and as the top panel of Fig. 3 shows, the changes in temperature and dew point across the analysis area are relatively small. Of kinematic importance, the mesonet data indicated an internal RFD outflow surge boundary behind the initial gust front similar to other recent mesonet data analysis (Finley and Lee 2004, Lee et al. 2004) and possibly similar to recent radar observations (Wurman et al. 2007). This surge appears juxtaposed with the tornado not unlike that detailed in Finley and Lee (2004).

As shown by MSR2002 and GLF2007, tornado likelihood and intensity appear related to thermodynamic characteristics of the RFD outflow. Since fluctuations in θ_v (from a base state) are proportional to buoyancy, θ_v' was analyzed to assess the buoyancy within the RFD outflow, some of which appears to be ingested into the tornado noting the radial storm-relative flow in the second panel of Fig. 3. θ_v departures from the base state are quite small from behind the initial gust front to just west and southwest of the tornado. Some of the "warmest" θ_v values are in and near the tornado. Thus, the magnitudes of the θ_v departures of the air south, east and within/near the tornado are consistent with those associated with tornado environments by MSR2002 and Grzych et. al. (2007). At the time of this analysis, the tornado is embedded in air having little negative buoyancy.

Given the focused mesonet sampling in the near-tornado and broader RFD outflow environment, a smaller region with a higher density of plotted observations was examined to construct the flow field in Fig. 4. The broader flow field reveals a generally diffluent RFD outflow with gradually cooler θ_v air being advected to the east and south in a storm-relative framework. Fortunately, M3 is close enough to the tornado to sample the induced radial flow as the vortex centroid passed by within 200-300 m to the north. Note that the edge of the circulation was substantially closer. Based on the implied flow field, parcels moving out of the RFD outflow just west of the tornado are moving into a confluent zone as they pass around and into the right side of the tornado. At this time, the near-tornado region

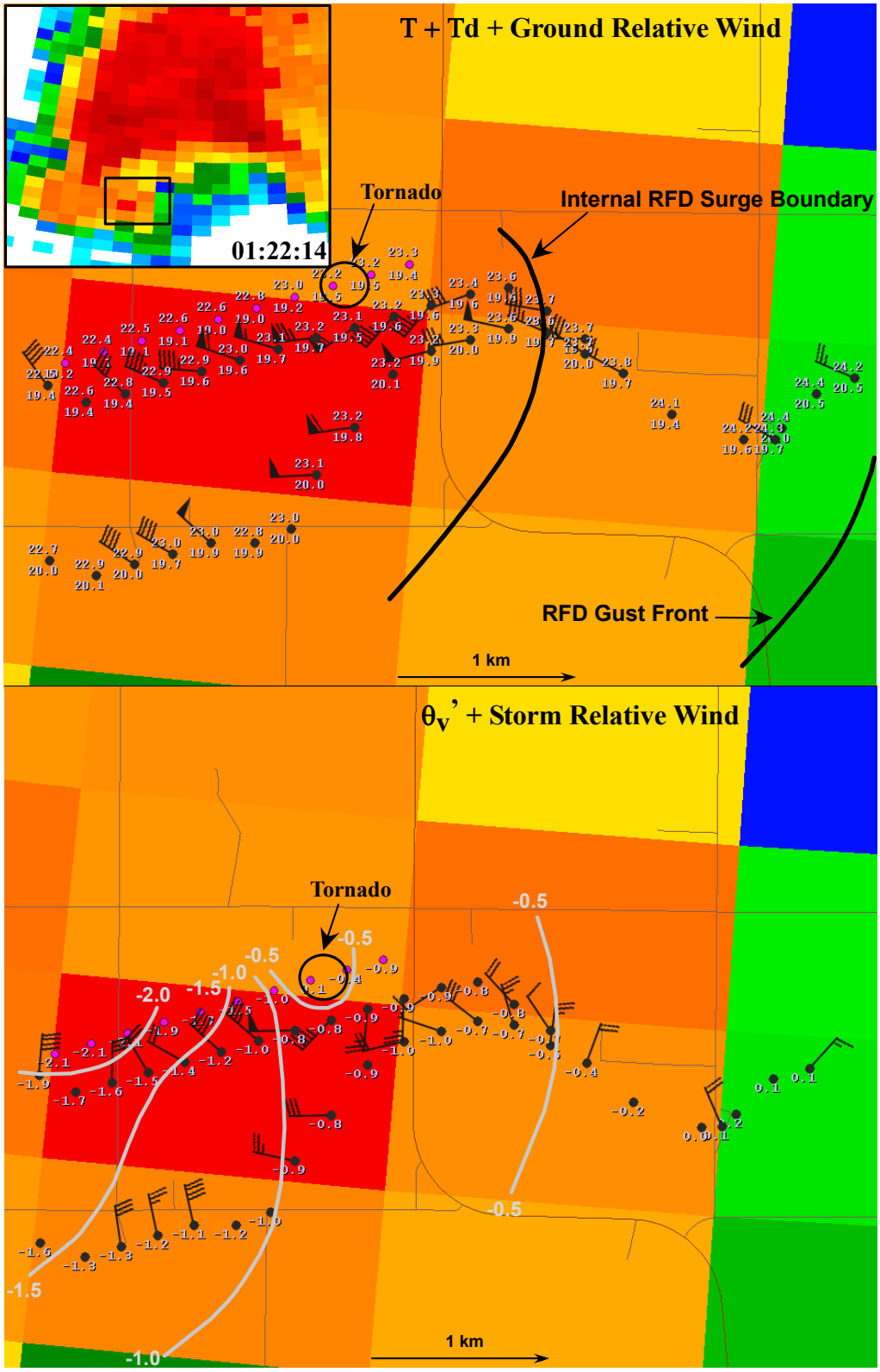

Fig. 3. Mesonet and probe positions with time-space conversion applied. Top right inset shows storm reflectivity structure at reference time with embedded inset showing the focused analysis domain. Top panel shows ground-relative velocity (kt) along with temperature (C), dewpoint (C) and subjective boundaries. Bottom panel depicts storm-relative winds (kt) along with θ_v' and contoured θ_v'. Probe 3 positions shown with magenta dots. Data are separated by 14 s. Stations with no staff had wind data removed in quality control.

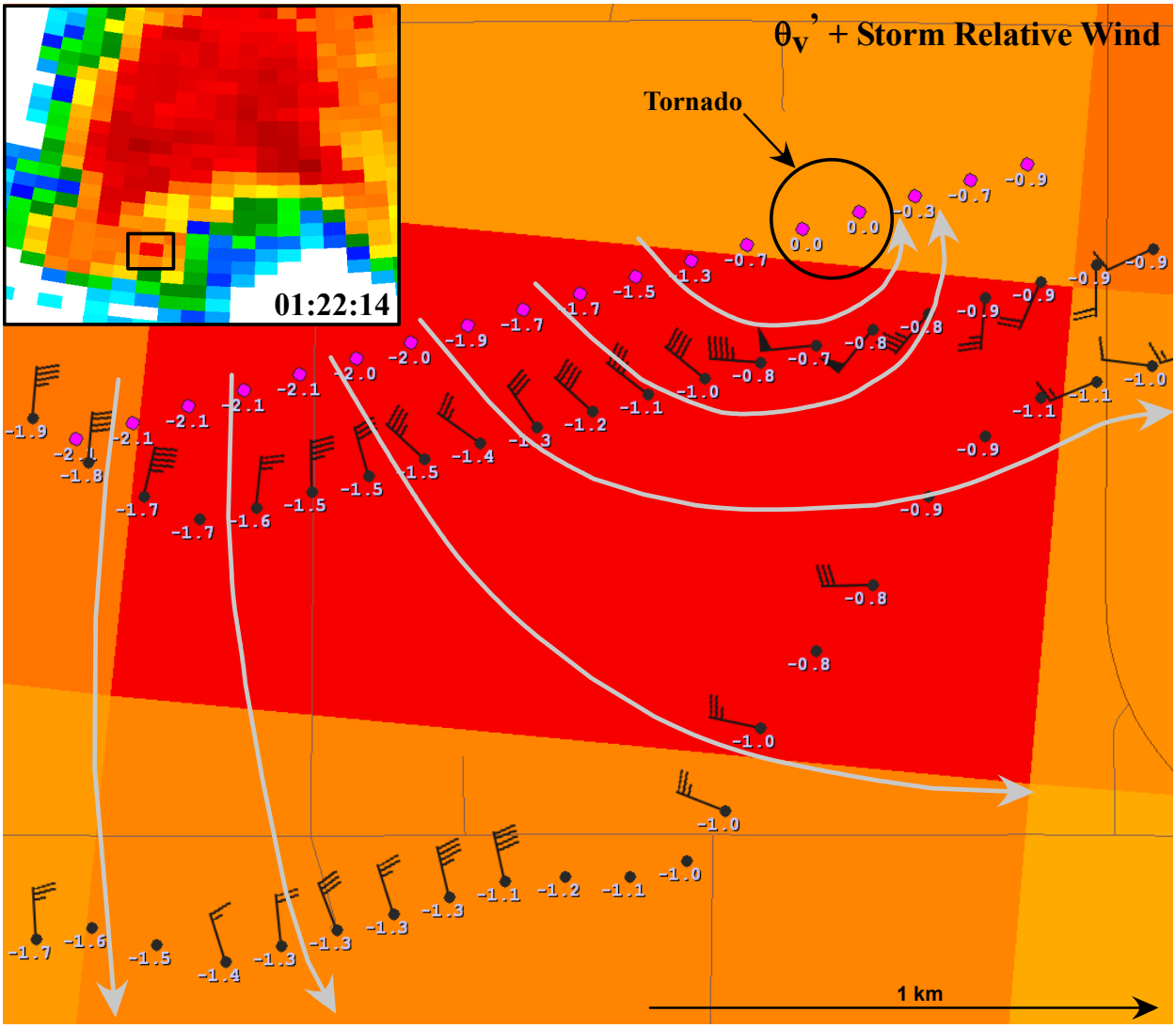

Fig. 4. As in Fig. 3 except data point spacing is 8 s and subjective streamlines are plotted. Embedded inset at the top right shows the focused area of this analysis. The tornado diameter approximates the actual width of the vortex.

and that area just east, and to a somewhat lesser extent, just south of the tornado, have the highest buoyancy (i.e., smallest negative buoyancy). The mapping clearly shows the most buoyant air lying closest to the tornado with parcels having low θ_v' values feeding into the tornado for a short duration. As noted in Fig. 3 and evident in Fig. 4, less buoyant air lies just west of the tornado and presumably northwest as well. With this flow field superposed on the θ_v' distribution, the air soon to be ingested into the tornado will be less buoyant. Interestingly, the tornado dissipated just several miles downstream of this position.

To further investigate the kinematic evolution of the flow sampled by M3, time series of storm-relative wind direction and speed along with ground relative speed are displayed in Fig. 5. The storm-relative inflow to the Tipton storm was striking with speeds averaging close to 50 kt. RFD gust front passage near 01:19:30 UTC brought a drastic drop to the storm-relative speeds given the similarity between the ground-relative winds and storm motion velocity vectors. Considerable storm-relative westerlies were sampled behind the internal RFD outflow surge boundary; however, at M3's location, the tornado-induced radial flow soon

backed the storm-relative flow as seen in Fig. 5 with winds directions commonly in the 180-210° range just preceding tornado passage. Storm-relative winds veer sharply as the tornado passes with marked wind speed ramps. While the peak 2 s storm-relative wind speed reaches 58 kt, the peak ground-relative speed at M3 was 86 kt. After tornado passage, storm-relative winds veer consistent with the diffluent pattern noted in Fig 4.

Time series of θ_v' shown in Fig. 6 depict a modest local maximum just behind the RFD gust front passage with gradually decreasing parcel buoyancy up to the time of tornado passage; however, θ_v' deficits of generally less than 1 K qualify this RFD outflow (during the analysis time interval) as being relatively "warm". Interestingly, the probe samples its warmest θ_v during the time of tornado passage with the mobile mesonet also recording θ_v increases although much smaller. Perhaps what the time series is showing is a different probe instrument response time than the mobile mesonet stations, or perhaps the very near and internal tornado environment is measurably different due to more substantial three-dimensional flow effects. After tornado passage the θ_v' time series for all stations continue to drop consistent with the gradually cooler pool of air noted to the west of the tornado in Fig. 3. The declining θ_v trend reflects a thermodynamically evolving RFD outflow that appears to be less supportive of tornado maintenance from a decreased buoyancy perspective. The outflow of this event never gets particularly cold by comparison with some of the RFD outflows documented in MSR2002. The evolving thermodynamic character of RFD outflows has been noted in MSR2002 and shown in thermodynamic time series in Lee et al. (2004) and Hirth et al. (2008).

Time series of θ_e' shown in Fig. 7 also reflects an RFD outflow environment that is thermodynamically favorable for tornadogenesis and maintenance. After a similar θ_e' local maximum measured just after the RFD gust front passage to that observed for θ_v' in Fig. 6, θ_e' drops to a quasi-steady level generally near -2 K up to and through the time of tornado passage. Once again, this thermodynamic signal is typical of RFD

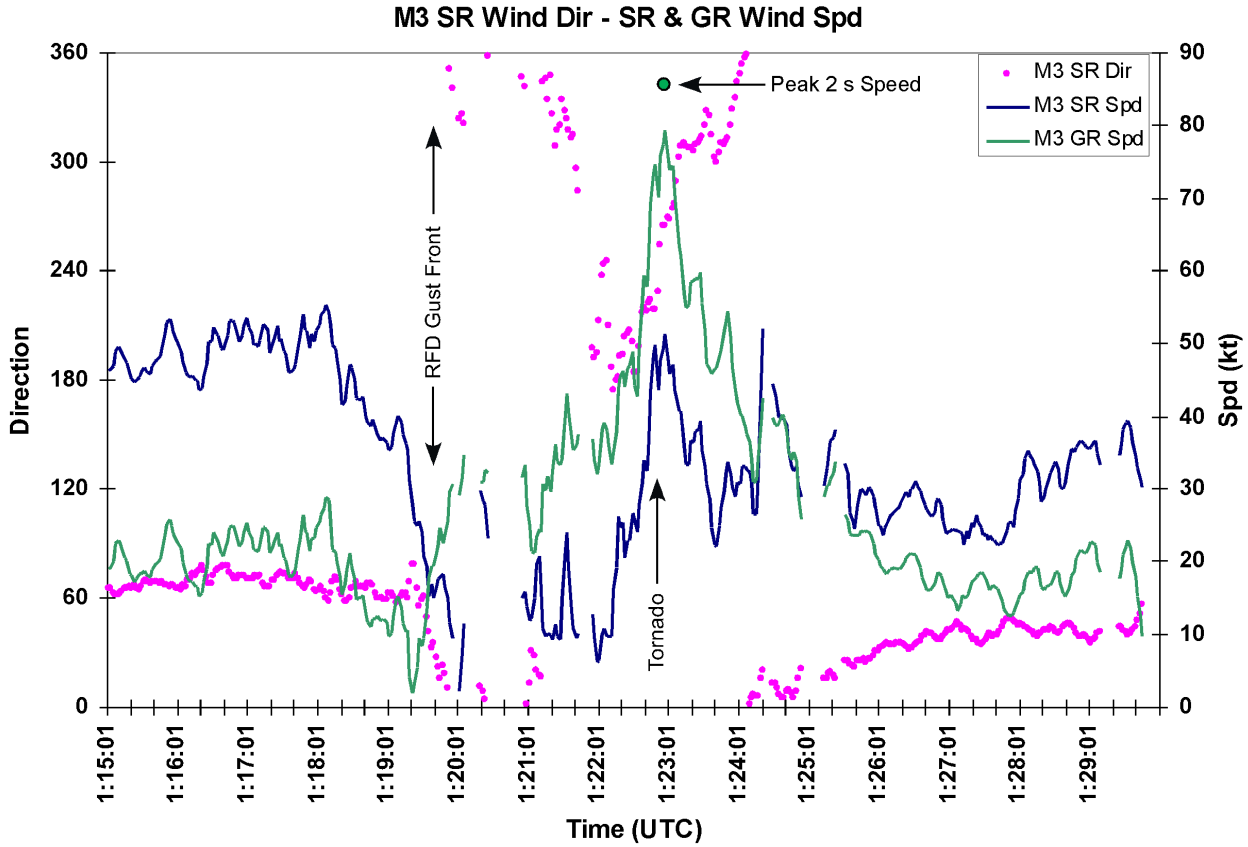

Fig. 5. Time series of storm-relative wind direction and storm-relative and ground-relative wind speed for the M3 station.

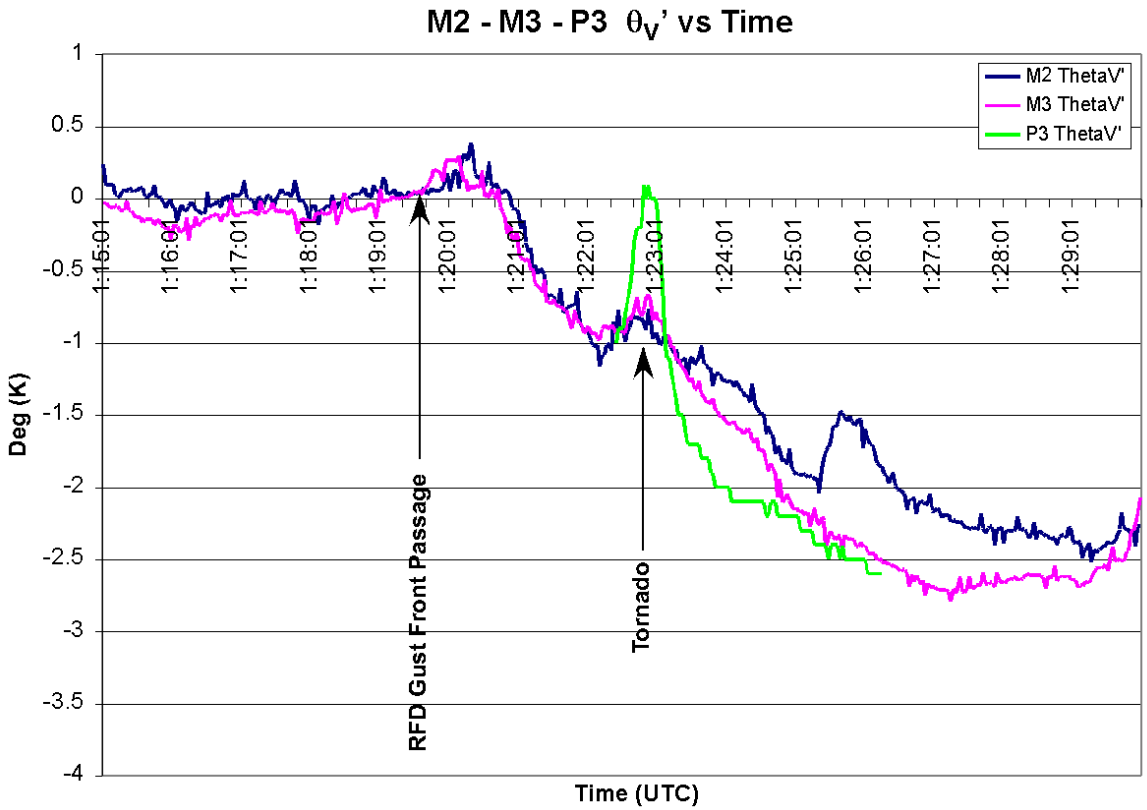

Fig. 6. Time series of θ_v' for the mobile mesonet stations (M2 and M3) and probe (P3).

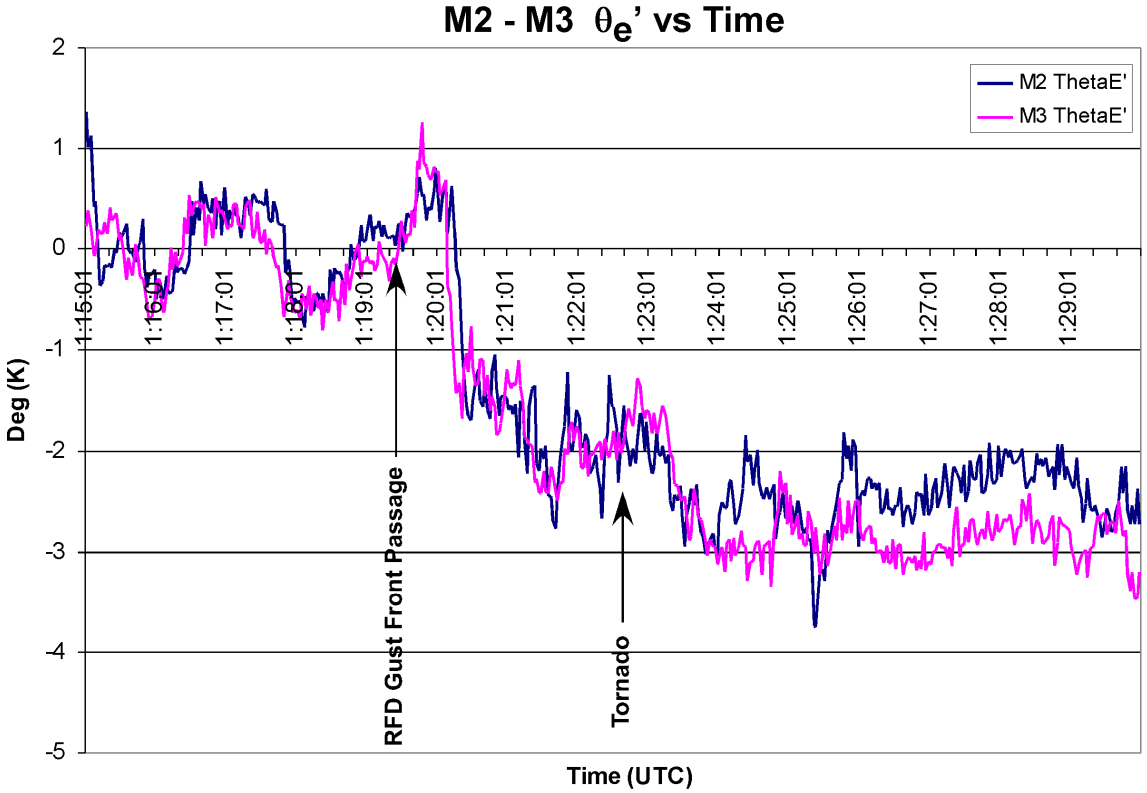

Fig. 7. Time series of θ_e' for the mobile mesonet stations (M2 and M3).

outflows documented in MSR2002 and GLF2007 that were associated with tornadic supercells

5. DISCUSSION

The dataset TWISTEX gathered on May 29 near Tipton, Kansas represents a unique opportunity to assess the thermodynamic characteristics of air parcels arriving at a tornado from areas within the RFD outflow. While the sampling array was not large enough to examine parcels moving into the tornado from its left (north) side, what can be said is that parcels residing at the tornado location and arriving at the tornado along its right flank were either only slightly negatively buoyant or very close to neutral as manifest in the mapped θ_v' field. While potential buoyancy within this region has yet to be analyzed since representative proximity soundings are in the process of being constructed, the small deficits of temperature and dew point from storm inflow values infers that these RFD parcels will likely have considerable positive potential buoyancy. More generally, in terms of the θ_v' and θ_e' analysis, the RFD outflow thermodynamic characteristics are consistent with those found by MSR2002 and GLF2007 that are associated with tornadic events.

An internal RFD surge boundary was present in the data that appeared to be largely a kinematic boundary given the similar thermodynamic properties and buoyancy characteristics of the air on either side. This interesting feature has been noted in other recent studies using a mobile mesonet (Finley and Lee 2004, Lee et al. 2004, Finley and Lee 2008) and appears to be juxtaposed with the tornadogenesis or tornado location. While there is a large range of thermodynamic gradients across this surge boundary between these cases, the common characteristic involves the air behind the surge having only weak negative buoyancy and likely possessing considerable potential buoyancy. With only a small number of documented cases of this internal RFD surge boundary, numerous other cases need to be gathered and analyzed to understand the kinematic and thermodynamic implications for tornadogenesis and maintenance.

The analysis presented here is still preliminary as work needs to be completed on mapping the potential buoyancy fields (CAPE), incorporating the southernmost in situ probe data and reviewing the thermodynamic and kinematic analysis and their inference and application to physical processes in storm/tornado evolution.

6. ACKNOWLEDGEMENTS

This research was supported by the National Geographic Society. The authors thank all TWISTEX 2008 participants for their contributions. Chris Karstens is recognized for numerous post-project conversations on case analysis and for assistance in data visualization. Carl Young was instrumental in assisting in probe deployment operations as well as in providing post-event consultation and video materials to the authors. Tony Laubach is recognized for helping manage mesonet field operations on May 29th and for his substantial contribution in getting video materials from a variety of sources to the authors. Patrick Skinner was a great help in consulting on post-project data quality control.

7. REFERENCES

Finley, C. A., and B. D. Lee, 2004: High resolution mobile mesonet observations of RFD surges in the June 9 Basset, Nebraska supercell during project answers 2003. Preprints*, 22nd Conf. on Severe Local Storms*, Hyannis, MA, Amer. Meteor. Soc., Conference CD-ROM,. P11.3.

Finley, C. A., and B. D. Lee, 2008: Mobile mesonet observations of an Intense RFD and multiple gust fronts in the May 23 Quinter, Kansas tornadic supercell during TWISTEX 2008. Electronic proceedings, *24th Conf. on Severe Local Storms,* Savannah, GA Amer. Meteor. Soc., P3.18.

Grzych, M. L., B. D. Lee, and C. A. Finley, 2007: Thermodynamic analysis of supercell rear-flank downdrafts from Project ANSWERS. *Mon. Wea. Rev.*, **135**, 240-246.

Hirth, B. D., J. L. Schroeder, and C. C. Weiss, 2008: Surface analysis of the rear-flank downdraft outflow in two tornadic supercells. *Mon. Wea. Rev*., **136**, 2344-2363.

Karstens, C. D., T. M. Samaras, A. Laubach, B. D. Lee, C. A. Finley, W. A. Gallus, F. L. Hann, 2008. TWISTEX 2008: In situ and mobile mesonet observations of tornadoes. Electronic proceedings, *24th Conf. on Severe Local Storms,* Savannah, GA Amer. Meteor. Soc., P3.11.

Lee, B. D., C. A. Finley, and P. Skinner, 2004: Thermodynamic and kinematic analysis of multiple RFD surges for the 24 June 2003 Manchester, South Dakota cyclic tornadic supercell during Project ANSWERS 2003. Preprints*, 22nd Conf. on Severe Local Storms*, Hyannis, MA, Amer. Meteor. Soc., CD-ROM, 11.2.

Markowski, P. M., 2002: Mobile mesonet observations on 3 May 1999. Wea. Forecasting, 17, 430-444.

Markowski, P. M., J. M. Straka, and E. N. Rasmussen, 2002: Direct surface thermodynamic observations within the rear-flank downdrafts of nontornadic and tornadic supercells. *Mon. Wea. Rev.,* **130**, 1692-1721.

Samaras, T.M., and J. J. Lee, 2003. Pressure measurements within a large tornado, *Proc. 84th American Meteorological Society Annual Meeting*, Seattle, WA.

Samaras, T. M., 2004: A historical perspective of in-situ observations within tornado cores. Preprints, *22nd Conf. on Severe Local Storms, Hyannis, MA, Amer, Meteor. Soc., CD_ROM,* P11.4.

Straka, J. M., E. N. Rasmussen, and S. E. Fredrickson, 1996: A mobile mesonet for fine-scale meteorological observations. *J. Atmos. Oceanic Technol*., **13**, 921-936.

Wurman, J., Y. Richardson, C. Alexander, S. Weygandt, P. F. Zhang, 2007: Dual-Doppler and single-Doppler analysis of a tornadic storm undergoing mergers and repeated tornadogenesis. *Mon. Wea. Rev*., **135**, 736-758.